Received: 17 February 2024 | Revised: 8 June 2024 | Accepted: 1 July 2024

DOI: 10.1111/jnc.16181

Journal of Neurochemistry JNC The Official Journal of the International Society for Neurochemistry WILEY

ORIGINAL ARTICLE

Special Issue: The Brain in Flux: Genetic, Physiologic, and Therapeutic Perspectives on Transporters in the Nervous System

# Role of palmitoylation on the neuronal glycine transporter GlyT2

R. Felipe[1] | J. Sarmiento-Jiménez[1] | E. Camafeita[2,3] | J. Vázquez[2,3] | B. López-Corcuera[1,4]

[1]Departamento de Biología Molecular, Instituto de Biología Molecular (IUBM), Centro de Biología Molecular Severo Ochoa, Consejo Superior de Investigaciones Científicas-Universidad Autónoma de Madrid, Madrid, Spain

[2]Centro Nacional de Investigaciones Cardiovasculares. (ISCIII), Madrid, Spain

[3]CIBER de Enfermedades Cardiovasculares (CIBERCV), Madrid, Spain

[4]IdiPAZ-Hospital Universitario La Paz, Madrid, Spain

**Correspondence**
B. López-Corcuera, Departamento de Biología Molecular, Instituto de Biología Molecular (IUBM), Centro de Biología Molecular Severo Ochoa, Consejo Superior de Investigaciones Científicas-Universidad Autónoma de Madrid, Madrid, Spain.
Email: beatriz.lopez@uam.es

**Funding information**
Fundación Ramón Areces, Grant/Award Number: CIVP20A6612; 'la Caixa' Foundation, Grant/Award Number: LCF/PR/HR22/52420019; NextGenerationEU/PRTR; MCIN/AEI/10.13039/501100011033, Grant/Award Number: CEX2020-001041-S, EQC2021-007053-P, PLEC2022-009235 and PLEC2022-009298; Comunidad de Madrid, Grant/Award Number: S2022/BMD-7333-CM (INMUNOVAR-CM); MCIN/AEI/10.13039/501100011033, Grant/Award Number: PID2020-119399RB-I00 and PID2021-122348NB-I00; European Regional Development Fund (ERDF) A way of making Europe

## Abstract

The neuronal glycine transporter GlyT2 removes glycine from the synaptic cleft through active $Na^+$, $Cl^-$, and glycine cotransport contributing to the termination of the glycinergic signal as well as supplying substrate to the presynaptic terminal for the maintenance of the neurotransmitter content in synaptic vesicles. Patients with mutations in the human GlyT2 gene (*SLC6A5*), develop hyperekplexia or startle disease (OMIM 149400), characterized by hypertonia and exaggerated startle responses to trivial stimuli that may have lethal consequences in the neonates as a result of apnea episodes. Post-translational modifications in cysteine residues of GlyT2 are an aspect of structural interest we analyzed. Our study is compatible with a reversible and short-lived S-acylation in spinal cord membranes, detectable by biochemical and proteomics methods (acyl-Rac binding and IP-ABE) confirmed with positive and negative controls (palmitoylated and non-palmitoylated proteins). According to a short-lived modification, direct labeling using click chemistry was faint but mostly consistent. We have analyzed the physiological properties of a GlyT2 mutant lacking the cysteines with high prediction of palmitoylation and the mutant is less prone to be included in lipid rafts, an effect also observed upon treatment with the palmitoylation inhibitor 2-bromopalmitate. This work demonstrates there are determinants of lipid raft inclusion associated with the GlyT2 mutated cysteines, which are presumably modified by palmitoylation.

**KEYWORDS**
cysteine, glycine, GlyT2, lipid rafts, palmitoylation, transporter

**Abbreviations:** ACN, acetonitrile; acyl-RAC, acyl-resin-assisted capture; GPCR, G-protein-coupled receptor; HAM, hydroxylamine; IP-ABE, immunoprecipitation and acyl-biotin-exchange; NEM, N-ethyl maleimide; RRID, Research Resource Identifier; SLC6, Solute Carrier 6; TCEP, Tris(2-carboxyethyl)phosphine; 17-ODYA, 17-octadecynoic acid.

R. Felipe and J. Sarmiento-Jiménez contributed equally to this work.

# 1 | INTRODUCTION

Glycine is the main inhibitory neurotransmitter in caudal areas of the central nervous system. Brainstem and spinal cord glycinergic pathways control muscle tone, motor rhythms, spinal reflex responses, and the processing of sensory and nociceptive information (Foster et al., 2015; Legendre, 2001). The neuronal glycine transporter GlyT2 removes glycine from the synaptic cleft through active $Na^+$, $Cl^-$, and glycine cotransport, and contributes to the termination of the glycinergic signal together with its glial counterpart GlyT1 (Marques et al., 2020). GlyT2 activity also supplies substrate to the low-affinity vesicular glycine transporter VIAAT and hence allows the maintenance of the glycine content in synaptic vesicles. Deletion of the GlyT2 gene in mice blocks glycinergic inhibition and reproduces the symptoms of a human disease called hyperekplexia (OMIM 149400) (Gomeza et al., 2003). Patients with certain mutations in the human GlyT2 gene (*SLC6A5*), develop the disease characterized by hypertonia and exaggerated startle responses to trivial stimuli and that may have lethal consequences in the neonates as a result of apnea episodes (Dreissen & Tijssen, 2012; López-Corcuera et al., 2019; Rees et al., 2006; Thomas et al., 2013).

GlyT2 belongs to the SLC6 family of neurotransmitter transporters, which also includes transporters for GABA and monoamines (Freissmuth et al., 2018). Structurally, these proteins contain cytoplasmic N- and C-termini and 12 transmembrane domains (TMs) connected by external and internal loops arranged into two topologically inverted repeats (Yamashita et al., 2005). During transport, the repeats are organized into two 4 TM bundles, rock one against the other exposing alternately substrate and ions to one side or the other of the membrane. This permits the protein structure to adopt outward, occluded, or inwardly directed conformational states. Models of GlyT2 were first based on the prokaryote ortholog LeuTAa (Yamashita et al., 2005) and later on data from eukaryote crystals or cryo-EM (Coleman et al., 2019; Nayak et al., 2023; Penmatsa et al., 2013; Shahsavar et al., 2021).

GlyT2 is a crucial protein for glycinergic inhibition and changes in its intracellular trafficking or transport activity must be fine tuned. Transporter traffic is mediated by clathrin (de Juan-Sanz et al., 2011; Fornes et al., 2008), and regulated by interaction with several partners: syntaxin 1 (Geerlings et al., 2001), the Rab11 protein (Núñez et al., 2009), and protein kinase C (Fornes et al., 2004; Fornes et al., 2008). GlyT2 transport activity is modulated by the $Na^+K^+$-ATPase (de Juan-Sanz et al., 2013); the plasma membrane $Ca^{2+}$ pump (PMCA) and the $Na^+Ca^{2+}$ exchanger (NCX) (de Juan-Sanz et al., 2014); and the purinergic and acetylcholine receptors (Jiménez et al., 2011, 2022; Villarejo-López et al., 2017). In addition, it has been proven that the transporter is post-translationally modified by phosphorylation by glycogen synthase kinase 3 (GSK3b) (Jiménez et al., 2015) and by ubiquitination by the E3 ubiquitin ligases (LNX1/2) (de la Rocha-Muñoz et al., 2019), and E3 ligases involved in the Hedgehog signaling pathway (de la Rocha-Muñoz et al., 2021). Besides, the lipid environment regulates the membrane distribution and glycine transport by GlyT2, which is located in lipid rafts (Núñez et al., 2008). Therefore, the regulatory procedures affecting GlyT2 traffic or activity are essential mechanisms to modulate its function and may have consequences in glycinergic neurotransmission physiology or pathologies.

One very frequent post-translational modification in synaptic proteins is S-palmitoylation, a reversible modification in which a palmitic acid is linked to a cysteine residue through a thioester bond (Yeste-Velasco et al., 2015). Palmitoylation is enzymatically catalyzed by palmitoyltransferases (PATs) also called DHHCs because of the sequence of its catalytic domain (Lobo et al., 2002). Twenty-three PATs have been identified in humans, which are membrane proteins mainly found in the Golgi, the ER, and some in the plasma membrane (Ohno et al., 2006). The modification is dynamic and can be removed by a small group of palmitoyl thioesterases: PPT1/2 and APT isoforms (Won et al., 2018).

Approximately 41% of the human palmitoylome is made up of proteins expressed at the synapse including integral membrane proteins such as GPCRs, AMPA, and glutamate receptor subunits and proteins localized in synaptic vesicles such as SNAP25, CSP, and synaptotagmin I (Sanders et al., 2015). The dopamine transporter DAT, which shares about 50% sequence identity with GlyT2, is palmitoylated (Rastedt et al., 2017). Palmitoylation can regulate multiple aspects of proteins, such as the intracellular trafficking, biogenesis, conformation of TMs, localization in lipid rafts, or other post-translational modifications such as phosphorylation or ubiquitination (Blaskovic et al., 2013; Jin et al., 2021; Zaballa & van der Goot, 2018). Alteration of the homeostatic balance of palmitoylation is involved in the pathogenesis of various neurological diseases, such as Alzheimer's disease (Andrew et al., 2017), Huntington's disease (Yanai et al., 2006), or X-related mental retardations in humans (Mansouri et al., 2005).

After isolation and proteomics analysis of brainstem and spinal cord palmitoylome, we identified the glycine transporter GlyT2 among the potentially palmitoylated proteins. In this report, we analyze whether the neuronal glycine transporter GlyT2 is palmitoylated using an array of different approaches. Our results are compatible with palmitoylation regulating the activity of GlyT2.

# 2 | METHODS

## 2.1 | Materials

Female 250–300 g Wistar rats (Charles River) were bred under standard conditions at the Centro de Biología Molecular Severo Ochoa (CBMSO) in accordance with procedures approved in the Directive 2010/63/EU of the European Union with approval of the Research Ethics Committee of the Universidad Autónoma de Madrid and the Dirección General de Agricultura, Ganadería y Alimentación of the Community of Madrid (Spain). Ethics approval reference number: PROEX 138.3/21. All the personnel managing the animals hold the required accreditation: Ref.: 10-3330-00674.7/2023. Rat housing was in type IV buckets (35 cm wide × 57 cm long × 10 cm high). Food and water were provided ad libitum. Five females coexisted per bucket. Rabbit and rat antibodies against the N-terminus of GlyT2 were generated in house (Nunez et al., 2009; Zafra et al., 1995). Other primary antibodies used were anti-transferrin receptor (Invitrogen #13–6800, RRID:AB_2533029), anti-GAPDH (Abcam Cat# ab8245, RRID:AB_2107448), mouse anti-calnexin (BD Biosciences Cat# 610523, RRID:AB_39788) anti-ubiquitin (Santa Cruz Biotechnology Cat# sc-8017, RRID:AB_628423), anti-α-tubulin (Sigma-Aldrich Cat# T6074, RRID:AB_477582), and anti-flotilin (BD Biosciences, Cat# 610821, RRID:AB_398140). The following compounds were from 17-Octadecynoic acid 17-ODYA (Cayman chemicals # 90270); Biotin-azide (Cayman chemicals, Cat# 13040); EZ-Link™ BMCC-Biotin (Thermo Fisher Scientific, Cat# 21900); EZ-Link™ Sulfo-NHS-SS-Biotin (Thermo Fisher Scientific, Cat# 21441); and Hydroxylamine (Alfa Aesar), Cat# A15398.36; Tyopropil sepharose 6B (Sigma–Aldrich). All other chemicals used were from Sigma–Aldrich unless otherwise noticed. Neurobasal medium and B27 supplement were purchased from Invitrogen.

## 2.2 | GlyT2 mutagenesis and transporter expression

GlyT2 substitution mutants were generated by site-directed mutagenesis using the commercial QuikChange Site-Directed Mutagenesis kit (Agilent Technologies, Cat#: 200519), and the rat GlyT2 in pcDNA3 as a template according to the manufacturer's instructions (Benito-Muñoz et al., 2018). The complete coding region of the constructs was sequenced to verify that only the desired mutation had been introduced. COS7 cells (American Type Culture Collection, RRID:CVCL_0224) were used. The COS7 cell line is not listed as a commonly misidentified cell line by the International Cell Line Authentication Committee (ICLAC; http://iclac.org/databases/cross-contaminations/). Cells were expanded and refrozen during the first passage. Aliquots were thawed and used below 30 passages. Cells were grown and transfected using TurboFect Transfection Reagent (Thermo Fisher Scientific, Cat#: R0532), following the manufacturer's protocol (2 μL reagent/μg of DNA). Cells were incubated for 48 h at 37°C until used (Arribas-Gonzalez et al., 2015).

## 2.3 | Obtaining samples enriched in rat spinal cord membranes (P2)

Sixty-day-old Wistar rats were killed using first $CO_2$ (97.2%) treatment for rapid loss of consciousness without hypoxia, followed by cervical dislocation. Brainstem and spinal cords were extracted and homogenized in ice-cold sucrose medium (0.32 M sucrose, 10 mM Hepes-NaOH, pH 7.4, 1 mM phenylmethylsulfonyl fluoride (PMSF), 1:200 protease inhibitor cocktail (Sigma–Aldrich, Cat# P7626 and *P8465*)), with a glass homogenizer (Wheaton). After centrifugation at 2000×*g* for 5 min, the supernatant was collected, the pellet was resuspended again in sucrose medium, and centrifugation was repeated. The two supernatants were mixed and concentrated by centrifugation at 10 000×*g* for 25 min. The obtained pellet was resuspended in HBM medium (20 mM HEPES-NaOH, pH 7.4; 140 mM NaCl, 5 mM KCl, 1 mM $MgCl_2$, 1.2 mM $Na_2HPO_4$, and 5 mM $NaHCO_3$). Membranes from three rats were used.

## 2.4 | [$^3$H]-glycine transport assays

COS7 cells were washed and incubated in phosphate-buffered saline (PBS) containing 2 μCi/mL [2-$^3$H]-glycine (1.6 TBq/mmol; PerkinElmer Life Sciences, Cat# NET004) at 10 μM final glycine concentration, if not otherwise stated (Benito-Muñoz et al., 2018). After 10 min, the reactions were terminated by aspiration, followed by PBS wash. Protein concentration (Bradford, Biorad) and [2-$^3$H]glycine (liquid scintillation, Opti-Fluor, PerkinElmer, LKB 1219 Rackbeta) were determined. Glycine accumulation by mock-transfected cells was subtracted from that of the transporter-transfected cells and normalized by the protein concentration. Kinetic analyses were performed by varying glycine concentration in the uptake medium between 0.5 and 500 μM and kinetic parameters were obtained after graph representation using GraphPad Prism 7® software.

## 2.5 | Surface biotinylation assays and western blot (WB)

Cells expressing the transporters were labeled with EZ-Link™ Sulfo-NHS-Biotin (1.0 mg/mL in PBS; Thermo Fisher Scientific, Cat#: 21217) at 4°C for 30 min, as described (Arribas-Gonzalez et al., 2015). After free biotin quenching with 100 mM L-lysine in PBS, cells were scrapped, and protein concentration was determined (Bradford). Equal amounts of proteins were lysed with RIPA buffer (1% Triton™ X-100, 0.1% SDS, 0.5% sodium deoxycholate, Tris–HCl 50 mM, NaCl 150 mM, 1 mM EDTA, 1 mM PMSF, and 1 : 200 protease inhibitor cocktail (PI), from Sigma–Aldrich, Cat# P7626 and P8465) during 30 min at 4°C. An aliquot of the lysate was saved (total protein), and the remainder was incubated with 50% streptavidin-agarose beads for 90 min at RT and centrifuged. Beads were washed 3 times with 1 mL RIPA and bound proteins (biotinylated) were eluted with 2× Laemmli buffer (65 mM Tris, 10% glycerol, 2.3% SDS, 100 mM DTT, 0.01% bromophenol blue) for 10 min at 75°C. Samples were run in SDS–PAGE using 4% and 6%–7.5% stacking and resolving gels, transferred to nitrocellulose membranes with a semi-dry transfer system (1.2 mA/cm$^2$, 90 min in 48 mM Tris, 40 mM glycine, 15% methanol, and 1.3 mM SDS). The blocking buffer was milk (Central Lechera Asturiana) at 4% in PBS (137 mM NaCl, 2.7 mM KCl, 10 mM $Na_2HPO_4$, and 1.8 mM $KH_2PO_4$, pH 7.4), and the washing buffer was PBS-Tween 20 (Sigma–Aldrich, Cat#: 8.22184.0500) at 0.05%. Bands were visualized by enhanced chemiluminescence detection (ECL, Bio-Rad). Linear range film exposures were imaged using a GS-900 calibrated imaging densitometer (Bio-Rad) and quantified using Image Lab Software (Bio-Rad).

## 2.6 | Ubiquitination assay

COS7 cells treated with 10 μM MG-132 (Hözel Biotech, Cat#: HY-13259C) for 3–4 h at 37°C, were 2× washed with PBS at 4°C, harvested using Ub buffer (50 mM Tris–HCl pH 7.5, 150 mM NaCl, 1 mM EDTA, and 50 mM N-ethyl maleimide (NEM) with PI) and cell protein content determined (de la Rocha-Muñoz et al., 2021). Equal amounts of protein were centrifuged, and pellets were resuspended in 90 μL of Ub buffer. Then, 10 μL of 10% SDS were added, and samples were incubated for 10 min at 95°C to disrupt protein interactions. Afterward, samples were diluted by adding 34 μL of Ub buffer containing 4% Triton X-100 and 1 mL of Ub buffer containing 1% Triton X-100. After 30 min on rotary shaking at 4°C, lysates were precleared with 50% Protein G-sepharose (PGS, Neo Biotech, Cat#: NB-45-00037-5) in Ub buffer for 30 min at 4°C and then overnight incubated with anti-GlyT2 antibody. Then, PGS was added for 90 min at RT followed by three washes with ice-cold Ub buffer and elution in 2× Laemmli buffer at 75°C for 15 min. Samples were subjected to 6% SDS–PAGE and WB with ubiquitin-specific antibodies and GlyT2 antibodies.

## 2.7 | Capture of palmitoylated proteins using resin (acyl-RAC)

Based on the method by (Forrester et al., 2011). Rat spinal cord membranes (P2) or COS7 cells were lysed in blocking buffer (100 mM HEPES-NaOH pH 7.5, 1 mM EDTA, 2.5% SDS, 10 mM Tris(2-carboxyethyl)phosphine (TCEP), 50 mM NEM and PI) by passing 5× through a 25G × 5/8″ needle and incubating at 37–40°C for 1 h with shaking. After centrifugation for 15 min at 20 000 × *g*, the supernatant was incubated overnight at −20°C together with four volumes of cold acetone and again centrifuged for 10 min at 4°C. Precipitated proteins were washed 3× with acetone at −20°C and resuspended in binding buffer (100 mM HEPES-NaOH pH 7.5, 1 mM EDTA, 1% SDS, and PI). When indicated, all the buffers were supplemented with 8 M urea. An aliquot of total protein was saved. The remaining was divided into two aliquots and incubated with a thiopropyl sepharose 6B resin (Sigma–Aldrich) in the presence of 1 M hydroxylamine (HAM, freshly prepared in $H_2O$ from HCl salt and brought to pH 7.5 with concentrated NaOH) or vehicle (negative control) for 2–3 h at RT with shaking. The resin was washed 3× with binding buffer and eluted with Laemmli buffer for 15 min at 75°C. Samples were analyzed by WB.

## 2.8 | Immunoprecipitation and acyl biotin exchange (IP-ABE)

Based on the original method of (Brigidi & Bamji, 2013). Rat spinal cord membranes (P2) or COS7 cells were lysed in lysis buffer (50 mM Tris–HCl pH 7.5, 150 mM NaCl, 10 mM TCEP, 50 mM NEM, 2.5% SDS and PI) for 30 min at 4°C and centrifuged for 15 min at 20 000 × *g*. The pellet was discarded. After saving an aliquot (total protein), the supernatant was diluted 25-fold with lysis buffer without SDS and incubated overnight with an anti-GlyT2 antibody at 4°C while shaking. The sample was divided into two equal aliquots and incubated with PGS for 90 min with shaking at 4°C. After three washes with RIPA buffer containing 1 M HAM or vehicle (negative control), samples were incubated for 1 h at RT, washed 3 x with RIPA pH 7.5, and 2× with RIPA pH 6.5. Each aliquot was incubated with 4 μM of the irreversible free sulfhydryl group reagent EZ-Link™ BMCC-Biotin (Thermo Fisher Scientific, Cat#: 21900) in RIPA buffer pH 6.5 during 1 h at RT. Finally, samples were washed 3× with RIPA pH 6.5, eluted in Laemmli buffer for 15 min at 75°C, and analyzed by WB using streptavidin-HRP (Sigma–Aldrich). Bands are compared with those obtained in parallel WBs with protein-specific antibodies.

## 2.9 | Metabolic labeling with 17-ODYA and detection by click chemistry

The 80% confluent COS7 cells were labeled with 100 μM octadecynoic acid (17-ODYA) (Cayman Chemical, Cat#: Cay90270-1) or vehicle (DMSO) in DMEM containing 1% BSA free of fatty acids (Sigma–Aldrich, Cat#: A8806) for 5 h. After PBS washing and lysis in RIPA buffer (free of EDTA but with PI) for 30 min at 4°C with rotation, cells were centrifuged to remove non-solubilized material. Solubilized proteins were precipitated with 4 volumes of methanol, 1.5 volumes of chloroform, and 3 volumes of water, allowed to stand, centrifuged at 5000 × *g* for 2 min, and the pellet washed with methanol. The supernatant was discarded, and the dried pellet was resuspended in 50 μL of a buffer containing 50 mM Tris–HCl and 1% SDS at pH 8. The following reagents were added to the sample to reach the indicated final concentrations: Tris[(1-benzyl-1H-1,2,3-triazol-4-yl)methyl]amine 100 μM (Sigma–Aldrich, Cat#: 678937), 1 mM $CuSO_4$, 1 mM TCEP, and 100 μM azido-biotin (Cayman Chemical, Cat#: 13040). The click reaction was allowed to take place for 30 min at RT in a rotary shaker. Then, proteins were re-precipitated as above to remove unbound azido-biotin traces and resuspended in RIPA with 0.1% SDS. An aliquot of each sample was saved (total) and the remainder was precleared by incubation with PGS for 30 min at 4°C. After centrifugation, the supernatant was collected and incubated with streptavidin-sepharose beads for 90 min at RT. The beads were washed 3× with RIPA containing 0.1% SDS and the proteins were eluted with Laemmli buffer for 10 min at 75°C. Samples were analyzed by WB.

## 2.10 | Proteomic assays

### 2.10.1 | In gel protein digestion

Protein samples in Laemmli buffer were subjected to SDS–PAGE following the one-step in-gel digestion (Bonzon-Kulichenko et al., 2011). The unseparated protein bands were visualized by

Coomassie staining, excised, cut into pieces (2×2 mm), and placed in Eppendorf tubes. Then the gel fragments were washed with water and dehydrated with 100% acetonitrile (ACN) prior to incubation with 10 mM dithiothretitol (DTT) or 10 mM TCEP in 25 mM ammonium bicarbonate (AB) for 1 h with agitation at RT. Thereafter the gel pieces were dehydrated again with 100% ACN and incubated with 50 mM iodoacetamide (IAM) in 25 mM AB for 1 h in the darkness with agitation. Finally, the fragments were dehydrated again with ACN and vacuum/dried. The samples were then added pig trypsin (Promega, Madison, WI, USA) in 50 mM AB 10%/ACN at a 1:40 (w/w) ratio and incubated overnight at 37°C with agitation. After collecting the supernatant, the gel pieces were incubated with 0.5% trifluoroacetic acid (TFA) for 1 h at RT, and the new supernatant was collected and mixed with the previous supernatant. The peptide samples were vacuum-dried, resuspended in 0.1% TFA, and desalted using MiniSpin™ columns (The Nest Group, Ipswich, MA, USA). The peptides were eluted with 50% ACN/0.1% TFA and vacuum-dried.

#### 2.10.2 | Liquid chromatography–tandem mass spectrometry analysis

Liquid chromatography–tandem mass spectrometry (LC–MS/MS) analysis was performed on an Easy nLC 1000 nano-HPLC (Thermo Scientific) coupled to an Orbitrap Fusion tribrid mass spectrometer (Thermo Scientific). The peptide samples were resuspended in 0.1% formic acid (FA), loaded onto a PepMap100 C18 LC pre-column (75 μm internal diameter, 2 cm length, Thermo Scientific), and resolved on a NanoViper PepMap 100 C18 LC analytical column (75 μm diameter, 50 cm length, Thermo Scientific) using a linear gradient of buffer B (8%–31% in 5 h; B, ACN 90%/FA 0.1%) at a 200 nL/min flow rate. Mass analysis was carried out following a data-dependent acquisition method: the full scan of precursor ions was done in the 390–1500 Th range using $5\times10^5$ automatic gain control and 50 ms maximum injection time at 120 000 resolution. Precursor ions were then isolated based on their intensity in a Top 20 mode to induce their fragmentation by higher-energy collisional dissociation using a normalized collision energy of 33%. The fragments thus generated were detected in the Orbitrap analyzer with 30 000 resolution. The precursor isolation window in the quadrupole was set to 1.5 Th and the dynamic exclusion was set to 40 s.

#### 2.10.3 | Peptide and protein identification

For peptide identification, the fragmentation spectra were analyzed using the SEQUEST HT search engine (Eng et al., 1994) implemented in the Proteome Discoverer 2.1 program (Thermo Scientific) (Orsburn, 2021). The assignment of peptide sequences was carried out by comparing the experimental fragmentation spectra with the fragmentations calculated in silico with either Rattus Norvegicus or Chlorocebus sabaeus Uniprot protein sequences (as of August 2021), both supplemented with rat GlyT2 sequence. The following search parameters were used: tryptic digestion with two maximum missed cleavage sites; 800 ppm and 0.02 Da precursor and fragment mass tolerance, respectively; variable Met oxidation (+15.99492), Cys carbamidomethylation (+57.02146), Cys alkylation with N-ethylmaleimide (+125.04768), and Cys palmitoylation (+238.22967). The corresponding inverted protein sequences were incorporated into the database for subsequent estimation of the false positive rate (FDR) for peptide identification, which was calculated using the probability ratio method (Martínez-Bartolomé et al., 2008) with a precursor ion mass tolerance post-filtering of 15 ppm (Bonzon-Kulichenko et al., 2015). A 1% FDR threshold was considered for the identification of peptides, which were assigned to the most probable protein proposed by Proteome Discoverer.

### 2.11 | Bioinformatic predictions

To predict the GlyT2 cysteines that could be palmitoylated, two computer tools were used that rely on the amino acid sequence of the protein as starting information. One software used was PalmPred (Kumari et al., 2014), whose model is based on support vector machines. The other tool used was CSS-Palm (different versions, including version 4.0) (Ren et al., 2008). CSS-Palm version 4.0 has an algorithm trained with a database containing 583 palmitoylation sites from 277 different proteins.

### 2.12 | Detergent-resistant membrane (DRM) isolation

Membrane domains resistant to the solubilization by Triton™ X-100 (lipid rafts) were isolated as described (Núñez et al., 2008). During the whole procedure, cell cultures were kept at 4°C. After cell scrapping and protein concentration determination (Bradford), samples containing an equal amount of protein were lysed in 50 mM Tris–HCl pH 7.5, 150 mM NaCl, 5 mM EDTA, and 1% Triton™ X-100 for 40 min in rotation. After centrifugation at 3000 rpm for 10 min, the precipitate was discarded, and the supernatant was centrifuged in a Beckman ultracentrifuge (TL-100) for 1 h at 4°C at 100 000×*g*. The supernatant (soluble fraction) and the pellet (DRM fraction) were separately resuspended in Laemmli loading buffer and analyzed in SDS–PAGE and WB.

### 2.13 | Statistical analysis and data representation

Sample size determination is based on the identification of an effect with a 95% confidence level (*Z* score 1.96). An empirical approach was used to determine normality and the number of samples needed to be used: the standard deviation was calculated in pilot studies and n was estimated for a *Z* score of 1.96 (95% confidence level) with an *E* value of 5 (margin of error; 5% chance of a false positive). The actual statistical formula was

$$n = \left(\frac{Z\sigma}{E}\right)^2.$$

The normality of the population was explored with Shapiro–Wilk test, setting a standard alpha value of 0.05. The sample passed the normality test with $p$ values greater than 0.05 and W values close to 0.9.

For the experimental settings, using Statgraphics, we calculated the sample size for the following conditions: The term beta (probability of a type-II-error) was set at 0.2 (20% chances of not detecting an existing significant difference), alpha was set at 0.05 (margin of error indicating that there is a 5% chance of finding a difference that is not true) and a detectable difference of 1.5 times sigma.

The design of statistical studies was based on Ahsanullah M. Kibria G and Shakil M (2014, February 18) Normal and Student's t Distributions and Their Applications. https://doi.org/10.2991/978-94-6239-061-4 and Sorzano, C. O. S. (2023, June 2). Statistical experiment design for animal research. https://doi.org/10.31219/osf.io/e9s25.

Statistical analysis of the data and graph representation was performed using GraphPad Prism 7® software. Student's *t*-test was applied to compare two experimental groups. Multiple comparisons of different conditions were performed using a two-tailed one-way analysis of variance with Dunnett's multiple comparisons test. No test for outliers was conducted. Mean values along with the standard error of the mean of at least three experiments were represented in the graphs.

## 3 | RESULTS

### 3.1 | GlyT2 appears in the palmitoylome of brainstem and spinal cord

We used the acyl-RAC method to capture palmitoylated proteins using thiopropyl sepharose 6B resin from a preparation from rat nervous tissue enriched in brainstem-and-spinal cord membranes

**TABLE 1** Proteins detected in the Acyl-RAC assay coupled to mass spectrometry.

| | | Peptides | | |
|---|---|---|---|---|
| Gen | Protein | Control | HAM | Enrichment |
| Atp2b2 | Calcium-transporting ATPase | 1 | 38 | 38 |
| Atp2a2 | Sarcoplasmic/endoplasmic reticulum calcium ATPase 2 | 1 | 23 | 23 |
| Syn1 | Synapsin-1 | 0 | 21 | ∞ |
| Ncam2 | Neural cell adhesion molecule 2 | 0 | 18 | ∞ |
| Atp2b3 | Calcium-transporting ATPase | 2 | 18 | 9 |
| Cax | Calnexin | 1 | 9 | 9 |
| Atp1a1 | Sodium/potassium-transporting ATPase subunit alpha-1 | 4 | 23 | 5,8 |
| Slc6a9 | Sodium- and chloride-dependent glycine transporter 1 | 1 | 5 | 5 |
| Vdac1 | Voltage-dependent anion-selective channel protein 1 | 2 | 9 | 4,5 |
| Gnao1 | Guanine nucleotide-binding protein G(o) subunit alpha | 5 | 19 | 3,8 |
| Slc1a2 | Excitatory amino acid transporter 2 | 4 | 15 | 3,8 |
| Slc6a5 | **Sodium- and chloride-dependent glycine transporter 2** | 4 | 15 | 3,8 |
| Atp1a2 | Sodium/potassium-transporting ATPase subunit alpha-2 | 13 | 48 | 3,7 |
| Snap25 | Synaptosomal-associated protein | 8 | 24 | 3 |
| Plp1 | Myelin proteolipid protein | 4 | 12 | 3 |
| Vamp1 | Vesicle-associated membrane protein 1 | 2 | 5 | 2,5 |

*Note*: Rat spinal cord membrane samples were subjected to Acyl-RAC. The eluted proteins were then digested with trypsin and analyzed by LC–MS/MS. The table shows the number of peptides detected for each protein in the control condition and in the condition with HAM. Only those proteins in which more than one peptide has been detected and whose enrichment in the condition with HAM compared to the control condition is greater than or equal to two times have been considered. The enrichment column represents the ratio between the peptides detected in the hydroxylamine condition versus the control condition.

(P2). The solubilized proteins, sequentially treated with the reducing agent TCEP and with NEM to block free thiol groups, were bound to the resin in the presence or absence of neutral HAM, a compound that specifically cleaves the thioester bonds which bind the acyl groups to the protein cysteines. Therefore, in the presence of HAM, palmitoylated proteins became bound to the resin. Eluted proteins were digested with trypsin and subjected to analysis by LC–MS/MS. Table 1 shows a list of the main proteins specifically retained by the resin after HAM treatment, showing the fold enrichment in relation to the control condition on the basis of the number of identified peptides. The vast majority of the proteins we identified have been detected in the palmitoylome of different species, and many, such as calnexin (Lynes et al., 2013), Ncam2 (Lievens et al., 2016), Gnao1 (Ping et al., 2021), or myelin proteolipid protein (Schneider et al., 2005) were experimentally validated as palmitoylated (database Swisspalm, Blanc et al., 2015). These results indicated that the acyl-RAC enrichment protocol was successful in enriching palmitoylated proteins. Of note, GlyT2 appeared among these proteins, being detected with 15 peptides in the HAM condition but only 4 in the control, an enrichment even higher than other bona fide palmitoylated proteins such as Snap25 (Yanai et al., 2006). See Table S1 and Figure S1 for detailed information on the identified GlyT2 peptides by mass spectrometry.

The binding of GlyT2 to the thiopropyl sepharose resin could be monitored by WB of the acyl-RAC fractions, and the transporter was only detected in the fraction bound to the resin in the presence of HAM, and not in its absence (Figure 1). The absence of signal in the control indicated that the blocking by NEM of the free –SH groups of the protein was effective. In addition, the signal detected after HAM incubation indicated that free –SH groups were generated by the reagent. Consistently, when the membranes were pretreated with DTT, a reducing agent more aggressive than TCEP that is known to hydrolyze thioester bonds, the amount of protein bound to the resin after HAM treatment was dramatically reduced (Ji et al., 2013; Song et al., 2009). Although these assays were performed in the presence of high concentrations of SDS (2.5%–1%), we wished to confirm the binding of GlyT2 to the thiopropyl sepharose resin was direct and not mediated trough a palmitoylated interactor. With this purpose, we performed the acyl-Rac assay in the presence of 8 M urea in all the buffers along the procedure (Figure 1b). GlyT2 was still detected in the fraction bound to the resin exclusively in the presence of HAM, suggesting direct binding of the transporter to the resin.

To confirm that the HAM treatment releases new free thiols, we used IP-ABE. Rat spinal cord membranes sequentially treated with TCEP and NEM as above, were immunoprecipitated with anti-GlyT2 antibody. The IP proteins were then treated with HAM (or vehicle) and incubated with a biotinylated compound that has the same chemistry (maleimide) as the reagent used to alkylate the thiols previously (NEM). Biotinylated proteins were then analyzed by WB using streptavidin-HRP. As seen in Figure 1c, a band around 100 kDa was observed only in the sample treated with HAM and not in the control condition, which corresponds to the band detected with a GlyT2 antibody. These results demonstrate that HAM effectively generates new thiols.

HAM is a reagent that specifically cleaves the thioester bond between palmitates and the thiol groups of cysteines under neutral pH conditions (Drisdel & Green, 2004). Although other lipid modifications, such as prenylation and myristoylation, are not attached by thioester bond, and HAM treatment does not cleave these groups, we wished to confirm that the sensitivity to HAM was because of the presence of palmitoylated groups. For this purpose, we tested whether the binding of GlyT2 to the thiopropyl sepharose resin was sensitive to 2-bromoplamitate (2-BP). This compound is a permeable and irreversible general inhibitor of palmitoyltransferases. Treatment with 2-BP produced a significant reduction of the fraction of GlyT2 bound to the acyl-Rac resin in the presence of HAM (Figure 2a). Furthermore, 2-BP also promoted a time- and dose-dependent inhibition of glycine transport by GlyT2, producing and strong reduction of the Vmax (5 times in 30 min at 50 μM) and inhibiting the transport with $EC_{50}$ = 50 μM (Figure 2b). This reduction was contributed by a decrease in the plasma membrane expression of the transporter,

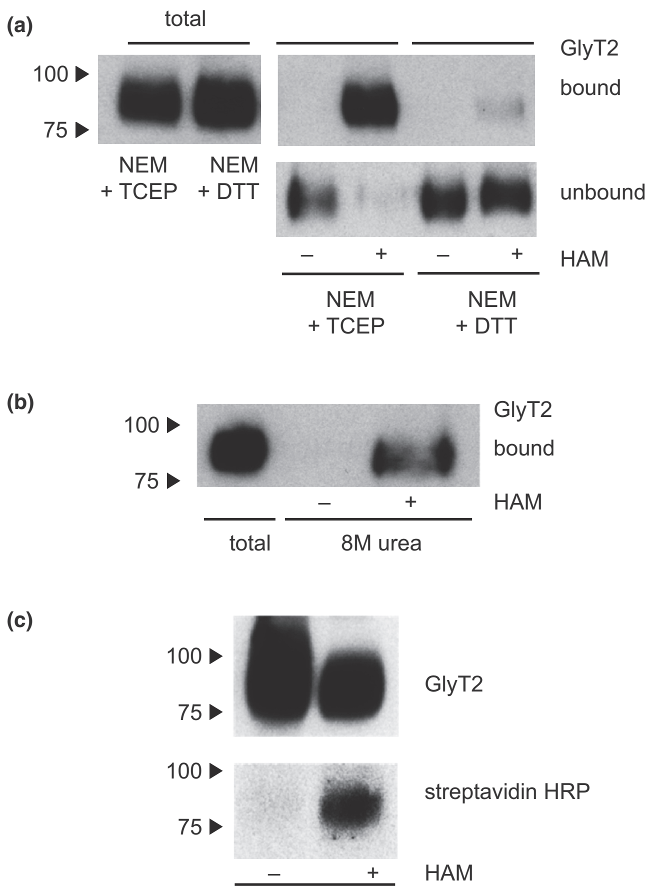


FIGURE 1 GlyT2 binds to thiopropyl sepharose resin in the presence of hydroxylamine. (a) Rat spinal cord membrane samples were pretreated with 10 mM TCEP or 10 mM DTT and they were subsequently subjected to acyl-RAC assay and analyzed by WB. (b) Samples enriched in rat spinal cord membranes were subjected to acyl-RAC assay in the presence of 8 M urea and then analyzed by WB as above. (c) Rat spinal cord membrane samples were subjected to IP-ABE assay and biotinylated proteins were detected by streptavidin-HRP (up) and GlyT2 protein using a specific antibody (down) (*n* = 4–10 independent cell culture preparations).

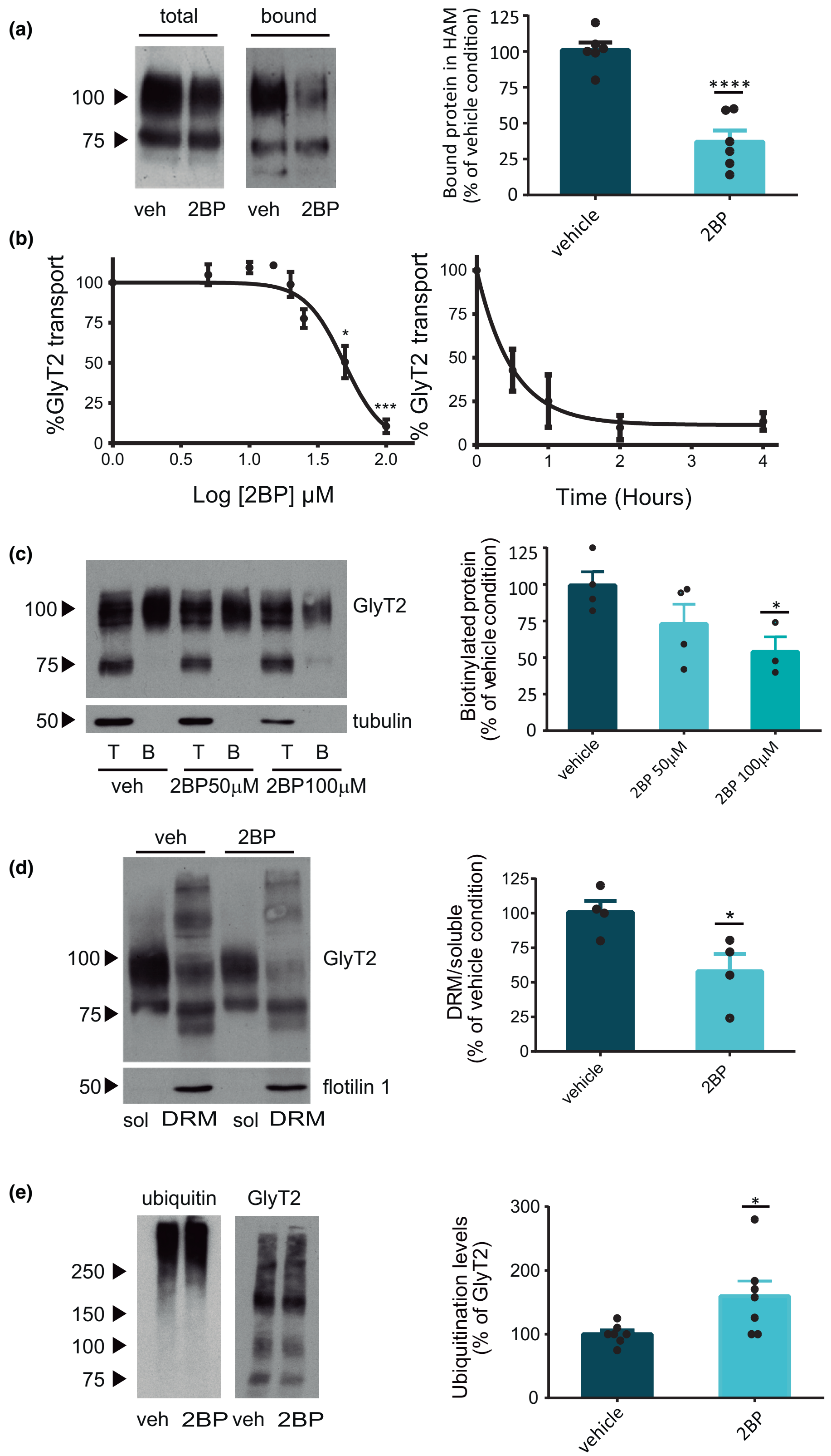


as monitored by surface biotinylation (50% decrease in 30 min at 100 μM) (Figure 2c), and also by a decrease in the capability of transporter inclusion in lipid rafts (Figure 2d). Moreover, 2-BP produced a significant increase in GlyT2 ubiquitination levels (Figure 2e), which is in good agreement with the inverse relationship between the levels of palmitoylation and ubiquitination that have been detected for many palmitoylated proteins (Blaskovic et al., 2013).

As GlyT2 was identified in indirect assays alongside palmitoylated proteins, we endeavored to directly detect palmitoylation of GlyT2 using the click chemistry method. To achieve this, COS7 cells

**FIGURE 2** Effect of 2-BP. (a) Treatment with 2-BP affects GlyT2 acyl-RAC behavior. COS7 cells expressing GlyT2 treated with vehicle or 100 μM 2-BP were subjected to acyl-RAC assay, and analyzed by WB. Right, quantification as a percentage of total GlyT2 bound to the resin in every condition. ****$p < 0.001$, significantly different from vehicle ($n = 6$ independent cell culture preparations). (b) Effect of 2-BP on the glycine transport by GlyT2. Glycine transport by GlyT2 expressed in COS7 cells was determined after treatment with 0, 1, 10, 15, 20, 25, 50, and 100 μM 2-BP for 30 min (left) or with 50 μM 2-BP for 0, 0.5, 1, 2, or 4 h (right). *$p < 0.05$, ***$p < 0.001$ significantly different from vehicle ($n = 4$ independent cell culture preparations). 100% glycine transport was 1.05 ± 6.1% nmol/mg protein/10 min. (c) Treatment with 2-BP reduces GlyT2 membrane expression. COS7 cells expressing GlyT2 treated with vehicle or 2-BP were subjected to biotinylation. Total (T, 3 μg) and biotinylated (B, 30 μg) fractions were analyzed by WB. Bar diagram depicts the percentage of total GlyT2, which is surface biotinylated. Tubulin was used as a loading control. *$p < 0.05$, significantly different from vehicle ($n = 4$ independent cell culture preparations). In vehicle condition, 41.1 ± 7.2% of the total transporter was biotinylated. (d) Treatment with 2-BP reduces GlyT2 in DRMs. COS7 cells expressing GlyT2 and treated with vehicle or 100 μM 2-BP were solubilized in a buffer containing 1% Triton™ X-100 and then centrifuged to separate the soluble (Sol) and the non-soluble fraction corresponding to detergent-resistant membranes (DRMs). Fractions were analyzed by WB with GlyT2 antibody. Flotilin1 was used as a lipid raft marker. The histogram depicts the ratio of the GlyT2 signal in the two fractions. *$p < 0.05$, significantly different from vehicle ($n = 4$ independent cell culture preparations). (e) Treatment with 2-BP increases GlyT2 ubiquitination. COS7 cells expressing GlyT2 were treated with vehicle or 10 μM MG132 and 50 μM 2-BP for 4 h and then subjected to WB with an anti-ubiquitin antibody and with an anti-GlyT2 antibody. Histogram: Quantification of the signal obtained with the antibody against ubiquitin normalized by the GlyT2-specific signal. *$p < 0.05$, significantly different from vehicle ($n = 7$ independent cell culture preparations).

transfected with GlyT2 were metabolically labeled with a palmitic acid analog containing an alkyne group (17-ODYA). The alkyne group can be conjugated with molecules containing an azide group through Huisgen cycloaddition (click chemistry) (Liao et al., 2021). Following cell lysis, the lysate underwent click chemistry using a biotin azide reagent. In this assay, proteins that had incorporated 17-ODYA would be labeled with biotin, and the biotinylated proteins were subsequently purified with streptavidin sepharose. As depicted in Figure 3a, GlyT2 was detected by WB in the biotinylated protein fraction in the cells incubated with 17-ODYA, but it was not detected in those incubated with the vehicle, suggesting 17-ODYA was incorporated into GlyT2.

## 3.2 | Cysteine substitution in GlyT2

We profited from the availability of GlyT2 cysteine substitution mutants (Gimenez et al., 2012) as well as generated new ones to obtain additional pieces of evidence on the transporter modification. GlyT2 is a 799 amino acid protein containing 22 cysteines in the rat sequence. Although there is not fully accepted consensus sequence for palmitoylation, we used two prediction softwares, PalmPred (Kumari et al., 2014) and CSS-Palm 4.0 (Ren et al., 2008; www.swisspalm.org), which highlighted 7 cysteines neighboring to the intracellular regions of the transporter (cysteines 3, 82, 509, 611, 612, 696, and 754). Alpha-fold GlyT2 homology model is shown in Figure 3b. Single mutants of these cysteines were expressed in COS7 cells and subjected to acyl-RAC assays (Figure 4a). Mutants C754S and C696S showed significantly lower retention in acyl-RAC in the presence of HAM. However, these two mutants showed wild-type phenotypes regarding glycine transport, surface expression, and ubiquitination level as did the rest of the mutants except for the mutant C509S (Figure 4b–e). Cysteine 509 is located at the proposed cholesterol site (Chater et al., 2023). Mutant C509S depicted altered features as compared to the wild-type (44.9 ± 9.3% glycine transport; 31.1 ± 6.5% surface expression; and increased ubiquitination, 163.3 ± 14%). This mutant showed retention along the secretory pathway since the proportion of mature transporters was significantly reduced to about 25% of the wild-type value. In addition, a trend toward reduction in surface expression was observed for C611S (Figure 4e), and mutant C754S showed a slightly diminished transport activity (Figure 4d). However, since C509S had a wild-type behavior in acyl-RAC experiments (Figure 4a), we disregarded its involvement as a palmitoylation site, despite it is possible that, even in our stringent conditions, a highly ubiquitinated mutant could have E3 ligases attached with a high affinity that could be retained by the acyl-RAC, and this may mask real binding of the mutant (Roth et al., 2006). Moreover, it is worth noting that all the cysteine mutants were sensitive to 2-BP, showing $EC_{50}$ in the 20–60 μM range, close to that of the wild-type.

## 3.3 | Characterization of the multiple cysteine mutants

The above results discarded the modification of one single cysteine but were compatible with more than one palmitoylated residue. Since Figure 4a showed acyl-RAC retention was reduced by mutation at either C696 or C754, although functional assays did not support these two cysteines as palmitoylation sites alone, we constructed three multiple mutants: a double mutant C696A/C754A (C2), a triple mutant C3A/C611A/C612A (C3), and a quintuple mutant, C5, in which all the cysteines with strong predictions by the two softwares were substituted (Cys3, 611, 612, 696, and 754; Figure 3b). The three multiple mutants showed significantly reduced binding to the thiopropyl sepharose resin as compared to the wild-type when tested in acyl-RAC experiments (60.9 ± 12.3% for C2; 62.6 ± 6.5% for C3; and 40.8 ± 15.2% for C5), (Figure 5a). The transport capability of the three mutants was reduced, which was more evident for the quintuple mutant (78.6 ± 7.0% for C2, 75.0 ± 6.3% for C3; and 63.5 ± 4.8% for C5 of the wild-type, Figure 5b). For the C2 and C3 mutants, the surface expression was largely consistent with the exhibited transport activity as detected in biotinylation experiments (Figure 5b). However, the glycine transport by the C5 mutant

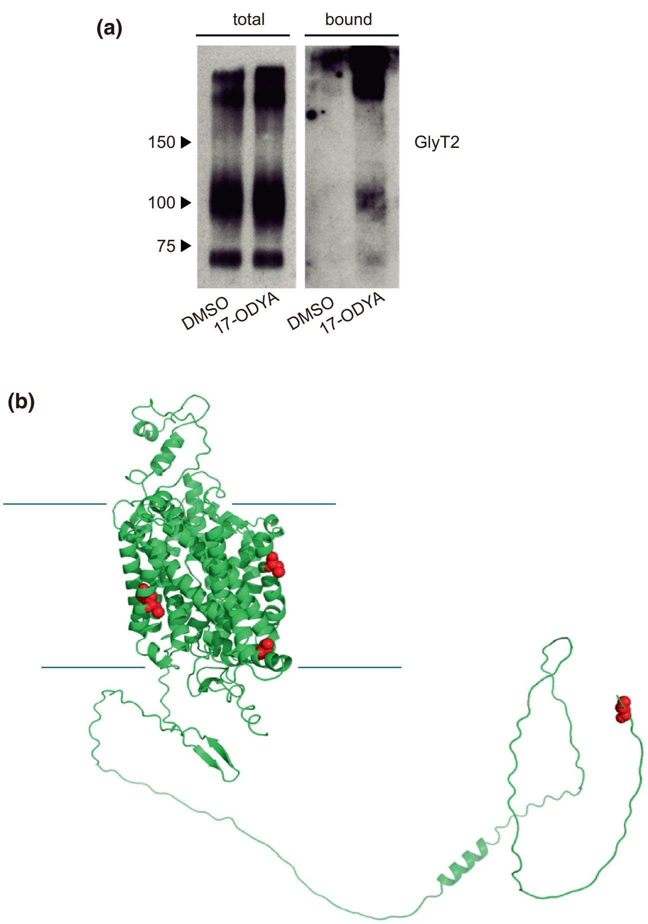


**FIGURE 3** GlyT2 is detected after metabolic labeling with 17-ODYA and click chemistry. (a) COS7 cells expressing GlyT2 were metabolically labeled with 100 μM 17-ODYA for 5 h, after which they were lysed, and a total protein fraction was extracted (total). The remainder of the lysate was precleared with PGS and biotinylated proteins were purified with streptavidin-agarose. Total, bound (biotinylated proteins), and prewash fractions were analyzed by WB using a specific anti-GlyT2 antibody ($n=4$ independent cell culture preparations). (b) Alpha-fold GlyT2 homology model. PyMol-generated GlyT2 lateral view is shown in a cartoon representation indicating as red spheres the cysteines with high prediction of palmitoylation, which were mutated in the quintuple mutant C5. The predicted extracellular and intracellular interfaces are also indicated.

was much lower than expected from its plasma membrane expression. This behavior indicated a deficiency in glycine transport of the plasma membrane resident transporter and not altered trafficking impairing the arrival to the plasma membrane. The reasons for such behavior might be diverse but since the plasma membrane GlyT2 prefers the lipid-ordered environment, it is a protein whose location in lipid rafts is necessary for optimal transport activity (Núñez et al., 2008), we measured the capability of lipid raft insertion of the mutants. To test this, COS7 cells expressing every mutant or the wild-type transporter were solubilized in the presence of Triton X-100™ and centrifuged to separate the soluble and insoluble fraction (DRMs, or lipid rafts). As shown in Figure 5c the C5 mutant was less prone to interact with lipid rafts than the wild type, since only 52.7 ± 16.2% of the mutant was found in DRMs. This behavior reminded the action of 2-BP, which, as already shown, reduced the presence of the transporter in lipid rafts by 58.3 ± 12.4% as compared to wild-type.

## 4 | DISCUSSION

Nervous tissue is particularly rich in palmitoylated proteins (Sanders et al., 2015). Many synaptic proteins including the SLC6 transporter of dopamine (DAT), and some GlyT2 interactors (PMCA, NCX, and CNX) are regulated by palmitoylation (Foster & Vaughan, 2011; Gök et al., 2020; Lynes et al., 2013; Yang et al., 2007). To investigate whether GlyT2 behaves as a palmitoylated protein, we isolated rat brainstem-spinal cord proteins through acyl-RAC, identified them using proteomics methods (LC–MS/MS), and found GlyT2 was detected among the isolated palmitoylome. In this study, we aimed to determine whether the transporter is modified and to establish the role of palmitoylation in GlyT2 regulation through various approaches. Initially, we used two biochemical assays based on the same chemistry, which reinforced one another: acyl-RAC and IP-ABE. Using these two indirect methods we detected the transporter together with the group of palmitoylated proteins from the brainstem-spinal cord. The biochemical controls implemented by us suggested the reduced free –SH groups of GlyT2 were fully blocked by NEM treatment since the transporter could not bind to

**FIGURE 4** Characterization of cysteine substitution mutants of GlyT2. (a) COS7 cells expressing the indicated transporters were subjected to Acyl-RAC assays. Total protein fractions and resin-bound fractions in the control condition (−) and HAM condition (+) were analyzed by WB using an anti-GlyT2 antibody. GAPDH was used as a positive control. Two gels were used to load the complete series of mutants. The histogram at right shows the quantification of the resin binding levels of the mutants as compared to the wild-type using the ratio between the fraction bound in the condition with HAM and the total fraction. **$p<0.01$, significantly different from the wild-type GlyT2 ($n=4$–7 independent cell culture preparations). (b) COS7 cells expressing either GlyT2 or the indicated cysteine mutants were lysed and analyzed by WB using an anti-GlyT2 antibody with tubulin as a loading control. The ratio of mature/immature transporter was quantified from similar blots and depicted in (c) ****$p<0.0001$ ($n=5$–10 independent cell culture preparations). (d) The cells were subjected to glycine transport assays for 10 min. 100% glycine transport was 1.2 ± 5.4% nmol/mg protein/10 min. **$p<0.01$ ($n=4$–7 independent cell culture preparations); or were subjected to surface biotinylation and then analyzed by WB (e) **$p<0.001$ ($n=4$–11 independent cell culture preparations); or were subjected to ubiquitination assay as in Figure 2 (f). For the wild-type, 48.1 ± 8.3% of the total GlyT2 transporter was biotinylated.

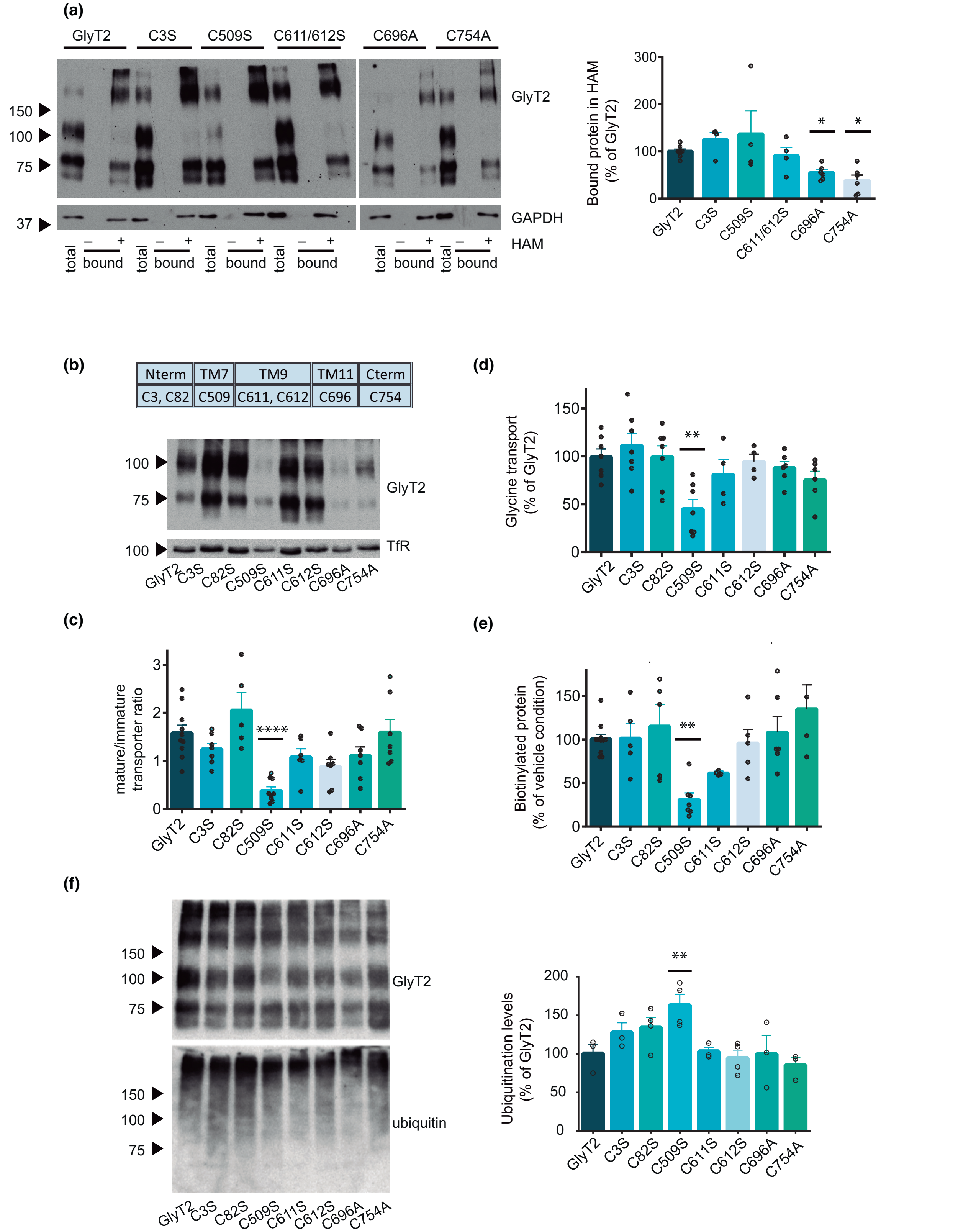


the thiopropyl sepharose (the acyl-RAC resin) in the absence of the thioester bond cleavage reagent HAM. HAM cleavage specifically affects the thioester bonds under neutral pH conditions (Drisdel & Green, 2004), generating new free –SH groups that allow binding to the resin. We proved the interaction of the transporter with the acyl-RAC resin was direct since even in the presence of 2.5% SDS and/or 8 M urea, the transporter was retained by the resin after HAM treatment and not in its absence. Additionally, the palmitoylation inhibitor 2-BP strongly reduced the binding of GlyT2 to the acyl-RAC resin.

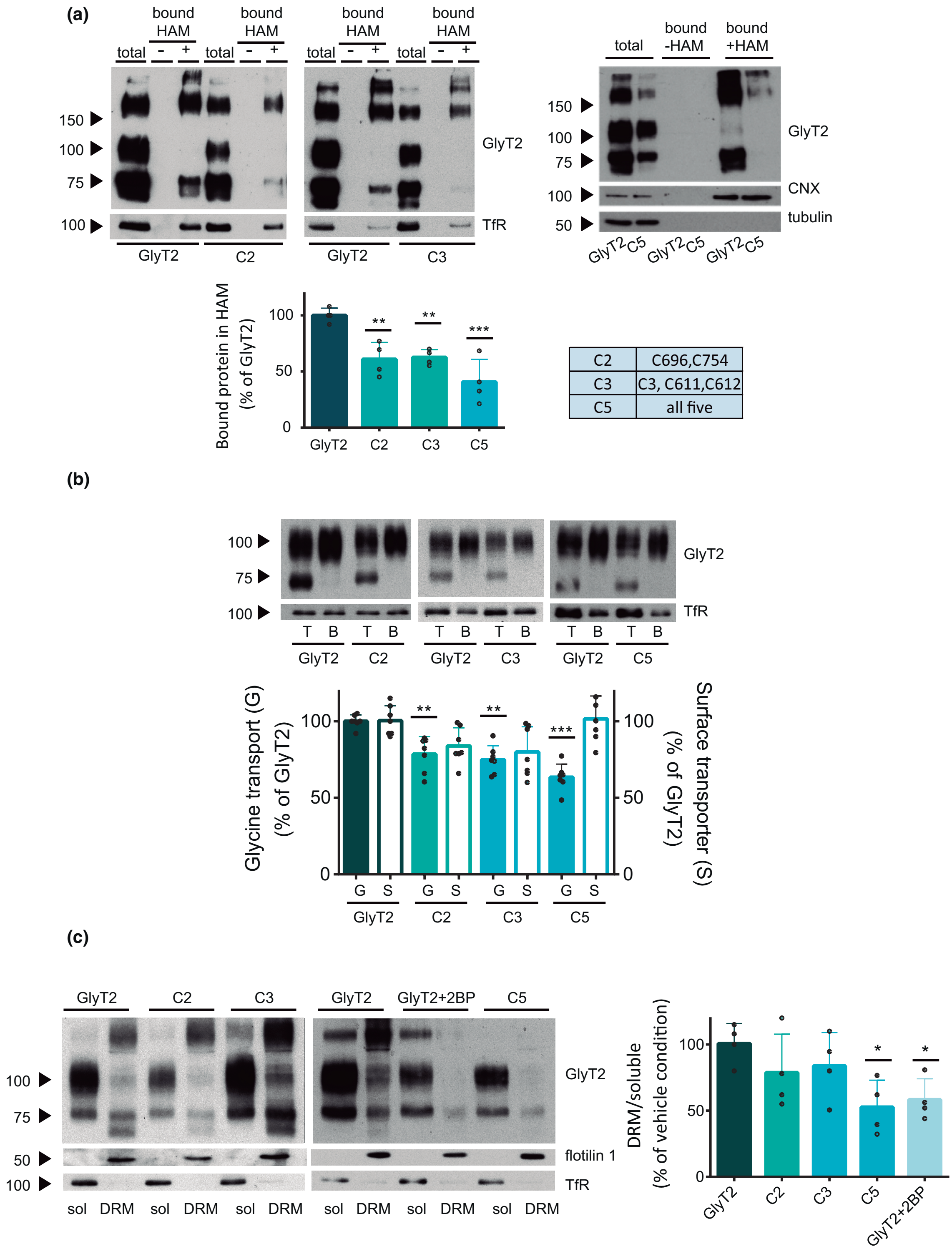


Further evidence supporting the sensitivity of GlyT2 to palmitoylation alterations is evident from the impact of 2-BP on GlyT2 function. This compound significantly inhibits GlyT2 transport, induces a moderate decrease in surface expression, diminishes lipid raft insertion, and leads to augmented ubiquitination. The measured glycine transport suggests that GlyT2 remaining at the plasma membrane after 2-BP treatment is not properly inserted in lipid rafts. This contributes to the high inhibition as GlyT2 requires lipid raft insertion for optimal transport activity (Núñez et al., 2008). 2-BP action suggests a multifaceted effect, despite the use of gentle treatments to minimize potential toxic effects. This complexity is understandable, given that the inhibitor may impact palmitoylated proteins, potentially influencing the biogenesis or interactions of the transporter (Blaskovic et al., 2013).

As further evidence for the modification, direct labeling of the transporter with 17-ODYA and click chemistry was achieved. This

**FIGURE 5** Characterization of the multiple cysteine mutants. (a) COS7 cells expressing the indicated multiple transporters subjected to Acyl-RAC assay. The samples were analyzed by WB and GlyT2 was detected with a specific antibody. Transferrin receptor (TfR) was used as a loading control. In the WB at right, the calnexin (CNX) signal was used as a positive control, and tubulin as a negative control. The histogram below shows the quantification of resin binding levels. $^{**}p<0.01$, $^{***}p<0.001$, significantly different from the wild-type ($n=4$ independent cell culture preparations). The substituted cysteines in each multiple mutants were shown in the right side table. (b) COS7 cells expressing the indicated transporters were subjected to surface biotinylation or glycine transport assay. T, total protein (3 μg) and B, biotinylated protein (9 μg). TfR, a membrane protein, was used as a loading control. The histogram below shows the quantification of glycine transport (solid bars, G) and surface biotinylation (open bars, S). $^{**}p<0.01$, $^{***}p<0.001$, significantly different from the wild-type GlyT2 ($n=7$ independent cell culture preparations). 100% glycine transport was 0.97 ± 4.0% nmol/mg protein/10 min. For the wild-type, 40.6 ± 9.7% of the total GlyT2 transporter was biotinylated, and 42.3 ± 12.3% for the C5 mutant. (c) The C5 mutant is less represented in lipid rafts. COS7 cells expressing GlyT2 treated with vehicle or 100 μM 2-BP, or transfected with the C5 mutant, were solubilized with a lysis buffer containing 1% Triton X-100™ and ultracentrifuged to separate the soluble fraction (Sol) and the detergent-resistant membranes (DRM) or lipid rafts. Fractions were analyzed by WB with a GlyT2 antibody. Flotlilin 1 and the TfR were used as markers of lipid rafts and non-rafts, respectively. The histogram at right shows the quantification of the GlyT2 signal in the non-soluble fraction versus that in the soluble fraction. $^{*}p<0.05$, significantly different from the untreated wild-type GlyT2 ($n=4$ independent cell culture preparations).

method was more convenient than [$^3$H]-palmitate labeling, which in our hands gave an extremely faint band after several months of film exposure. The click chemistry method gave a weak yet consistent labeling of GlyT2 that was not observed when 17-ODYA was absent from the incubation media, supporting the specificity of 17-ODYA incorporation to GlyT2. Of note, we also performed different trials using fluorescent-azide instead of biotin-azide to detect GlyT2 by gel fluorescence. However, no specific fluorescent signal was detected, neither for GlyT2 nor for other positive palmitoylation control proteins such as DAT and calnexin (Foster & Vaughan, 2011; Lynes et al., 2013), suggesting there was a methodological difficulty we were not able to solve. In any case, if the transporter is immersed in a dynamic palmitoylation process, robust direct labeling is not expected, and our data may be compatible with a reversible and short half-life GlyT2 palmitoylation.

Although in this work we present evidence supporting GlyT2 is palmitoylated, we should note that we were unable to detect a palmitoilated peptide using a proteomics approach. Directly detecting the palmitoyl moiety for any palmitoylated protein by mass spectrometry poses challenges, a common occurrence in the literature. Notably, only approximately one-third of verified palmitoylated proteins have been successfully identified as such through mass spectrometry. Palmitoylated peptides prove elusive during mass spectrometry analysis because of the tendency of the modification to be lost during sample handling or chromatographic procedures. Moreover, the high hydrophobicity of palmitoylated peptides complicates their detection under standard conditions for other peptides, necessitating meticulous optimization of solution gradients during chromatography (Ji et al., 2013). Despite our attempts to adjust gradients, detecting palmitoylated peptides remained elusive. An additional challenge arose from the limited sequence coverage of GlyT2. Given its status as an integral membrane protein, a portion of its sequence resides within the lipid layer. This structural characteristic hampers accessibility for digestion enzymes, resulting in a reduced number of peptides obtained. Furthermore, the identification of highly hydrophobic peptides from transmembrane sequences poses inherent difficulties (Eichacker et al., 2004). While we made efforts to enhance digestion by employing enzymes other than trypsin, like chymotrypsin and a combination of both, these modifications did not significantly improve GlyT2 coverage (data not shown).

The characterization of the GlyT2 single mutants of the cysteines highlighted by the palmitoylation prediction softwares did not enable the identification of a single modified residue. This led us to construct multiple mutants. Two mutants with two (C2) or three (C3) substituted cysteines showed slightly reduced glycine transport but were devoid of remarkable phenotype. However, the substitution of all five predicted cysteines (3, 611, 612, 696, and 754) in the C5 mutant, produced a phenotype that may be compatible with the modification. Nevertheless, we must say that the main target cysteines of PATs are usually intracellular or juxtamembrane cysteines and this location is only fulfilled by two out of the three cysteines included in the quintuple mutant. However, considering that for several proteins palmitoylation is controlled or interfered with by TM residues either as a signaling mechanism or through blocking the access of PATS, our data are consistent with some of the mutated cysteines being responsible for the observed phenotype, although perhaps not through the same mechanism (Vardar et al., 2022). One additional cysteine (799) was predicted by one of the palmitoylation softwares (www.swisspalm.org). This residue is part of the PDZ binding domain present in the C-terminal region of GlyT2, which regulates the trafficking and localization of the transporter at the synapse (Armsen et al., 2007). We tested a PDZ deletion mutant we previously generated and found it exhibits about 95% glycine transport and surface expression and displayed a phenotype close to the wild-type, leading us to disregard its consideration as a modification site.

The quintuple mutant (C5) could mimic the behavior of unmodified GlyT2. It exhibited decreased binding to the acyl-RAC resin, reduced transport activity, and diminished capability of lipid raft insertion. These features were also observed for GlyT2 under 2-BP treatment. According to 2-BP action, it was expected that palmitoylation stabilizes the function of the lipid raft-embedded transporter. Since the C5 mutant exhibited wild-type surface expression, its decreased glycine transport capability could be attributed to its reduced lipid raft inclusion. Indeed both, transport activity and lipid raft insertion, were quantitatively reduced to a similar extent in this

Journal of Neurochemistry JNC —WILEY

mutant. These findings suggest a role for palmitoylation in the localization of GlyT2 to lipid rafts. Our results contribute to the growing body of evidence implicating palmitoylation in the regulation of membrane protein localization (Blaskovic et al., 2013; Levental et al., 2010).

## 5 | CONCLUSIONS

In this study, we isolated the palmitoylome of rat brainstem-spinal cord and identified through proteomics methods (LC–MS/MS) the neuronal glycine transporter GlyT2 among the palmitoylated proteins. GlyT2 was detected in indirect (acyl-RAC and IP-ABE) and direct palmitoylation detection assays (17-ODYA labeling and click chemistry), fulfilling the experimental requirements for a palmitoylated protein. In addition, we accumulated evidence supporting the regulation of GlyT2 by palmitoylation. GlyT2 is sensitive to the palmitoyltransferase inhibitor 2-BP, which inhibits GlyT2 transport, surface expression, and lipid raft insertion, besides increasing ubiquitination. The substitution of 5 cysteines of GlyT2 reduces acyl-RAC retention and hinders lipid-raft insertion, besides reducing glycine transport as does the treatment with 2-BP. This work demonstrates there are determinants of lipid raft inclusion associated with the GlyT2 mutated cysteines, which are presumably modified by palmitoylation.

## AUTHOR CONTRIBUTIONS

**R. Felipe:** Methodology; investigation; formal analysis. **J. Sarmiento-Jiménez:** Investigation; methodology; formal analysis. **E. Camafeita:** Investigation; writing – original draft; writing – review and editing; formal analysis; software; supervision; methodology. **J. Vázquez:** Investigation; writing – original draft; writing – review and editing; software; formal analysis; supervision; funding acquisition; project administration. **B. López-Corcuera:** Conceptualization; funding acquisition; writing – original draft; writing – review and editing; project administration; supervision; investigation; validation.

## ACKNOWLEDGMENTS

This work was supported by MCIN/AEI/10.13039/501100011033, grant number PID2020-119399RB-I00 to B.L.-C.; the Fundación Ramón Areces, grant number CIVP20A6612 to B.L.-C.; an institutional grant from the Fundación Ramón Areces to the CBMSO; grant EQC2021-007053-P funded by MCIN/AEI/10.13039/501100011033 and by NextGenerationEU/PRTR; grant PID2021-122348NB-I00 funded by MCIN/AEI/10.13039/501100011033 and by "European Regional Development Fund (ERDF) A way of making Europe"; grants PLEC2022-009298 funded by MCIN/AEI/10.13039/501100011033 and by "European Union NextGenerationEU/PRTR"; grant PLEC2022-009235 funded by MCIN/AEI/10.13039/501100011033 and by "European Union NextGenerationEU/PRTR"; grant S2022/BMD-7333-CM (INMUNOVAR-CM) funded by Comunidad de Madrid; and "la Caixa" Foundation under the project code LCF/PR/HR22/52420019. The CBMSO is a Severo Ochoa Center of Excellence (CEX2021-001154-S). The CNIC is supported by the Instituto de Salud Carlos III (ISCIII), the Ministerio de Ciencia e Innovación (MCIN) and the Pro CNIC Foundation, and is a Severo Ochoa Center of Excellence (grant CEX2020-001041-S funded by MICIN/AEI/10.13039/501100011033). The authors wish to thank Enrique Núñez for their excellent technical assistance and support.

## CONFLICT OF INTEREST STATEMENT

The authors declare no conflicts of interest.

## PEER REVIEW

The peer review history for this article is available at https://www.webofscience.com/api/gateway/wos/peer-review/10.1111/jnc.16181.

## DATA AVAILABILITY STATEMENT

The data that support the findings of this study are available from the corresponding author upon reasonable request.

## ORCID

*B. López-Corcuera* https://orcid.org/0000-0002-0383-4241

## REFERENCES

Andrew, R. J., Fernandez, C. G., Stanley, M., Jiang, H., Nguyen, P., Rice, R. C., Buggia-Prévot, V., De Rossi, P., Vetrivel, K. S., Lamb, R., Argemi, A., Allaert, E. S., Rathbun, E. M., Krause, S. V., Wagner, S. L., Parent, A. T., Holtzman, D. M., & Thinakaran, G. (2017). Lack of BACE1 S-palmitoylation reduces amyloid burden and mitigates memory deficits in transgenic mouse models of Alzheimer's disease. *Proceedings of the National Academy of Sciences of the United States of America*, *114*(45), E9665–E9674. https://doi.org/10.1073/pnas.1708568114

Armsen, W., Himmel, B., Betz, H., & Eulenburg, V. (2007). The C-terminal PDZ-ligand motif of the neuronal glycine transporter GlyT2 is required for efficient synaptic localization. *Molecular and Cellular Neurosciences*, *36*(3), 369–380. https://doi.org/10.1016/j.mcn.2007.07.011

Arribas-Gonzalez, E., de Juan-Sanz, J., Aragon, C., & Lopez-Corcuera, B. (2015). Molecular basis of the dominant negative effect of a glycine transporter 2 mutation associated with hyperekplexia. *The Journal of Biological Chemistry*, *290*(4), 2150–2165. https://doi.org/10.1074/jbc.M114.587055

Benito-Muñoz, C., Perona, A., Abia, D., Dos Santos, H. G., Nunez, E., Aragon, C., & Lopez-Corcuera, B. (2018). Modification of a putative third sodium site in the glycine transporter GlyT2 influences the chloride dependence of substrate transport. *Frontiers in Molecular Neuroscience*, *11*, 347. https://doi.org/10.3389/fnmol.2018.00347

Blanc, M., David, F., Abrami, L., Migliozzi, D., Armand, F., Bürgi, J., & van der Goot, F. G. (2015). SwissPalm: Protein palmitoylation database. *F1000Research*, *4*, 261. https://doi.org/10.12688/f1000research.6464.1

Blaskovic, S., Blanc, M., & van der Goot, F. G. (2013). What does S-palmitoylation do to membrane proteins? *The FEBS Journal*, *280*(12), 2766–2774. https://doi.org/10.1111/febs.12263

Bonzon-Kulichenko, E., Garcia-Marques, F., Trevisan-Herraz, M., & Vázquez, J. (2015). Revisiting peptide identification by high-accuracy mass spectrometry: Problems associated with the use of narrow mass precursor windows. *Journal of Proteome Research*, *14*(2), 700–710. https://doi.org/10.1021/pr5007284

Bonzon-Kulichenko, E., Pérez-Hernández, D., Núñez, E., Martínez-Acedo, P., Navarro, P., Trevisan-Herraz, M., Ramos, M. D. C., Sierra, S., Martínez-Martínez, S., Ruiz-Meana, M., Miró-Casas, E., García-Dorado, D., Redondo, J. M., Burgos, J. S., & Vázquez, J. (2011). A robust method for quantitative high-throughput analysis of proteomes by $^{18}O$ labeling. *Molecular & Cellular Proteomics: MCP*, *10*(1), M110.003335. https://doi.org/10.1074/mcp.M110.003335

Brigidi, G. S., & Bamji, S. X. (2013). Detection of protein palmitoylation in cultured hippocampal neurons by immunoprecipitation and acyl-biotin exchange (ABE). *Journal of Visualized Experiments*, *72*, 50031.

Chater, R. C., Quinn, A. S., Wilson, K., Frangos, Z. J., Sutton, P., Jayakumar, S., Cioffi, C. L., O'Mara, M. L., & Vandenberg, R. J. (2023). The efficacy of the analgesic GlyT2 inhibitor, ORG25543, is determined by two connected allosteric sites. *Journal of Neurochemistry*. https://doi.org/10.1111/jnc.16028

Coleman, J. A., Yang, D., Zhao, Z., Wen, P.-C., Yoshioka, C., Tajkhorshid, E., & Gouaux, E. (2019). Serotonin transporter-ibogaine complexes illuminate mechanisms of inhibition and transport. *Nature*, *569*(7754), 141–145. https://doi.org/10.1038/s41586-019-1135-1

de Juan-Sanz, J., Nunez, E., Villarejo-Lopez, L., Perez-Hernandez, D., Rodriguez-Fraticelli, A. E., Lopez-Corcuera, B., Vazquez, J., & Aragon, C. (2013). $Na^+/K^+$-ATPase is a new interacting partner for the neuronal glycine transporter GlyT2 that downregulates its expression in vitro and in vivo. *The Journal of Neuroscience*, *33*(35), 14269–14281. https://doi.org/10.1523/JNEUROSCI.1532-13.2013

de Juan-Sanz, J., Nunez, E., Zafra, F., Berrocal, M., Corbacho, I., Ibanez, I., Arribas-Gonzalez, E., Marcos, D., Lopez-Corcuera, B., Mata, A. M., & Aragon, C. (2014). Presynaptic control of glycine transporter 2 (GlyT2) by physical and functional association with plasma membrane $Ca^{2+}$-ATPase (PMCA) and $Na^+$-$Ca^{2+}$ exchanger (NCX). *The Journal of Biological Chemistry*, *289*(49), 34308–34324. https://doi.org/10.1074/jbc.M114.586966

de Juan-Sanz, J., Zafra, F., López-Corcuera, B., & Aragón, C. (2011). Endocytosis of the neuronal glycine transporter GLYT2: Role of membrane rafts and protein kinase C-dependent ubiquitination. *Traffic*, *12*(12), 1850–1867. https://doi.org/10.1111/j.1600-0854.2011.01278.x

de la Rocha-Muñoz, A., Núñez, E., Arribas-González, E., López-Corcuera, B., Aragón, C., & de Juan-Sanz, J. (2019). E3 ubiquitin ligases LNX1 and LNX2 are major regulators of the presynaptic glycine transporter GlyT2. *Scientific Reports*, *9*(1), 14944. https://doi.org/10.1038/s41598-019-51301-x

de la Rocha-Muñoz, A., Núñez, E., Vishwanath, A. A., Gómez-López, S., Dhanasobhon, D., Rebola, N., López-Corcuera, B., de Juan-Sanz, J., & Aragón, C. (2021). The presynaptic glycine transporter GlyT2 is regulated by the hedgehog pathway in vitro and in vivo. *Communications Biology*, *4*(1), 1197. https://doi.org/10.1038/s42003-021-02718-6

Dreissen, Y. E., & Tijssen, M. A. (2012). The startle syndromes: Physiology and treatment. *Epilepsia*, *53*(Suppl 7), 3–11. https://doi.org/10.1111/j.1528-1167.2012.03709.x

Drisdel, R. C., & Green, W. N. (2004). Labeling and quantifying sites of protein palmitoylation. *BioTechniques*, *36*(2), 276–285. https://doi.org/10.2144/04362RR02

Eichacker, L. A., Granvogl, B., Mirus, O., Müller, B. C., Miess, C., & Schleiff, E. (2004). Hiding behind hydrophobicity. Transmembrane segments in mass spectrometry. *The Journal of Biological Chemistry*, *279*(49), 50915–50922. https://doi.org/10.1074/jbc.M405875200

Eng, J. K., McCormack, A. L., & Yates, J. R. (1994). An approach to correlate tandem mass spectral data of peptides with amino acid sequences in a protein database. *Journal of the American Society for Mass Spectrometry*, *5*(11), 976–989. https://doi.org/10.1016/1044-0305(94)80016-2

Fornes, A., Nunez, E., Alonso-Torres, P., Aragon, C., & Lopez-Corcuera, B. (2008). Trafficking properties and activity regulation of the neuronal glycine transporter GLYT2 by protein kinase C. *The Biochemical Journal*, *412*(3), 495–506. https://doi.org/10.1042/BJ20071018

Fornes, A., Nunez, E., Aragon, C., & Lopez-Corcuera, B. (2004). The second intracellular loop of the glycine transporter 2 contains crucial residues for glycine transport and phorbol ester-induced regulation. *The Journal of Biological Chemistry*, *279*(22), 22934–22943. https://doi.org/10.1074/jbc.M401337200

Forrester, M. T., Hess, D. T., Thompson, J. W., Hultman, R., Moseley, M. A., Stamler, J. S., & Casey, P. J. (2011). Site-specific analysis of protein S-acylation by resin-assisted capture. *Journal of Lipid Research*, *52*(2), 393–398. https://doi.org/10.1194/jlr.D011106

Foster, E., Wildner, H., Tudeau, L., Haueter, S., Ralvenius, W. T., Jegen, M., Johannssen, H., Hösli, L., Haenraets, K., Ghanem, A., Conzelmann, K.-K., Bösl, M., & Zeilhofer, H. U. (2015). Targeted ablation, silencing, and activation establish glycinergic dorsal horn neurons as key components of a spinal gate for pain and itch. *Neuron*, *85*(6), 1289–1304. https://doi.org/10.1016/j.neuron.2015.02.028

Foster, J. D., & Vaughan, R. A. (2011). Palmitoylation controls dopamine transporter kinetics, degradation, and protein kinase C-dependent regulation. *The Journal of Biological Chemistry*, *286*(7), 5175–5186. https://doi.org/10.1074/jbc.M110.187872

Freissmuth, M., Stockner, T., & Sucic, S. (2018). SLC6 transporter folding diseases and pharmacochaperoning. *Handbook of Experimental Pharmacology*, *245*, 249–270. https://doi.org/10.1007/164_2017_71

Geerlings, A., Nunez, E., Lopez-Corcuera, B., & Aragon, C. (2001). Calcium- and syntaxin 1-mediated trafficking of the neuronal glycine transporter GLYT2. *The Journal of Biological Chemistry*, *276*(20), 17584–17590. https://doi.org/10.1074/jbc.M010602200

Gimenez, C., Perez-Siles, G., Martinez-Villarreal, J., Arribas-Gonzalez, E., Jiménez, E., Nunez, E., de Juan-Sanz, J., Fernandez-Sanchez, E., Garcia-Tardon, N., Ibanez, I., Romanelli, V., Nevado, J., James, V. M., Topf, M., Chung, S. K., Thomas, R. H., Desviat, L. R., Aragon, C., Zafra, F., … Lopez-Corcuera, B. (2012). A novel dominant hyperekplexia mutation Y705C alters trafficking and biochemical properties of the presynaptic glycine transporter GlyT2. *The Journal of Biological Chemistry*, *287*(34), 28986–29002. https://doi.org/10.1074/jbc.M111.319244

Gök, C., Plain, F., Robertson, A. D., Howie, J., Baillie, G. S., Fraser, N. J., & Fuller, W. (2020). Dynamic palmitoylation of the sodium-calcium exchanger modulates its structure, affinity for lipid-ordered domains, and inhibition by XIP. *Cell Reports*, *31*(10), 107697. https://doi.org/10.1016/j.celrep.2020.107697

Gomeza, J., Ohno, K., Hulsmann, S., Armsen, W., Eulenburg, V., Richter, D. W., Laube, B., & Betz, H. (2003). Deletion of the mouse glycine transporter 2 results in a hyperekplexia phenotype and postnatal lethality. *Neuron*, *40*(4), 797–806.

Ji, Y., Leymarie, N., Haeussler, D. J., Bachschmid, M. M., Costello, C. E., & Lin, C. (2013). Direct detection of S-palmitoylation by mass spectrometry. *Analytical Chemistry*, *85*(24), 11952–11959. https://doi.org/10.1021/ac402850s

Jiménez, E., Fornés, A., Felipe, R., Núñez, E., Aragón, C., & López-Corcuera, B. (2022). Calcium-dependent regulation of the neuronal glycine transporter GlyT2 by M2 muscarinic acetylcholine receptors. *Neurochemical Research*, *47*(1), 190–203. https://doi.org/10.1007/s11064-021-03298-x

Jiménez, E., Nunez, E., Ibanez, I., Zafra, F., Aragon, C., & Gimenez, C. (2015). Glycine transporters GlyT1 and GlyT2 are differentially modulated by glycogen synthase kinase 3beta. *Neuropharmacology*, *89*, 245–254. https://doi.org/10.1016/j.neuropharm.2014.09.023

Jiménez, E., Zafra, F., Perez-Sen, R., Delicado, E. G., Miras-Portugal, M. T., Aragon, C., & Lopez-Corcuera, B. (2011). P2Y purinergic regulation of the glycine neurotransmitter transporters. *The Journal of*

*Biological Chemistry*, *286*, 10712–10724. https://doi.org/10.1074/jbc.M110.167056
Jin, J., Zhi, X., Wang, X., & Meng, D. (2021). Protein palmitoylation and its pathophysiological relevance. *Journal of Cellular Physiology*, *236*(5), 3220–3233. https://doi.org/10.1002/jcp.30122
Kumari, B., Kumar, R., & Kumar, M. (2014). PalmPred: An SVM based palmitoylation prediction method using sequence profile information. *PLoS One*, *9*(2), e89246. https://doi.org/10.1371/journal.pone.0089246
Legendre, P. (2001). The glycinergic inhibitory synapse. *Cellular and Molecular Life Sciences*, *58*(5–6), 760–793.
Levental, I., Grzybek, M., & Simons, K. (2010). Greasing their way: Lipid modifications determine protein association with membrane rafts. *Biochemistry*, *49*(30), 6305–6316. https://doi.org/10.1021/bi100882y
Liao, L. M. Q., Gray, R. A. V., & Martin, D. D. O. (Directors). (2021). Optimized incorporation of alkynyl fatty acid analogs for the detection of fatty Acylated proteins using click. *Chemistry*. https://doi.org/10.3791/62107
Lievens, P. M.-J., Kuznetsova, T., Kochlamazashvili, G., Cesca, F., Gorinski, N., Galil, D. A., Cherkas, V., Ronkina, N., Lafera, J., Gaestel, M., Ponimaskin, E., & Dityatev, A. (2016). ZDHHC3 tyrosine phosphorylation regulates neural cell adhesion molecule palmitoylation. *Molecular and Cellular Biology*, *36*(17), 2208–2225. https://doi.org/10.1128/MCB.00144-16
Lobo, S., Greentree, W. K., Linder, M. E., & Deschenes, R. J. (2002). Identification of a Ras palmitoyltransferase in Saccharomyces cerevisiae. *The Journal of Biological Chemistry*, *277*(43), 41268–41273. https://doi.org/10.1074/jbc.M206573200
López-Corcuera, B., Arribas-González, E., & Aragón, C. (2019). Hyperekplexia-associated mutations in the neuronal glycine transporter 2. *Neurochemistry International*, *123*, 95–100. https://doi.org/10.1016/j.neuint.2018.05.014
Lynes, E. M., Raturi, A., Shenkman, M., Ortiz Sandoval, C., Yap, M. C., Wu, J., Janowicz, A., Myhill, N., Benson, M. D., Campbell, R. E., Berthiaume, L. G., Lederkremer, G. Z., & Simmen, T. (2013). Palmitoylation is the switch that assigns calnexin to quality control or ER $Ca^{2+}$ signaling. *Journal of Cell Science*, *126*(Pt 17), 3893–3903. https://doi.org/10.1242/jcs.125856
Mansouri, M. R., Marklund, L., Gustavsson, P., Davey, E., Carlsson, B., Larsson, C., White, I., Gustavson, K.-H., & Dahl, N. (2005). Loss of ZDHHC15 expression in a woman with a balanced translocation t(X;15)(q13.3;cen) and severe mental retardation. *European Journal of Human Genetics: EJHG*, *13*(8), 970–977. https://doi.org/10.1038/sj.ejhg.5201445
Marques, B. L., Oliveira-Lima, O. C., Carvalho, G. A., de Almeida Chiarelli, R., Ribeiro, R. I., Parreira, R. C., da Madeira Freitas, E. M., Resende, R. R., Klempin, F., Ulrich, H., Gomez, R. S., & Pinto, M. C. X. (2020). Neurobiology of glycine transporters: From molecules to behavior. *Neuroscience and Biobehavioral Reviews*, *118*, 97–110. https://doi.org/10.1016/j.neubiorev.2020.07.025
Martínez-Bartolomé, S., Navarro, P., Martín-Maroto, F., López-Ferrer, D., Ramos-Fernández, A., Villar, M., García-Ruiz, J. P., & Vázquez, J. (2008). Properties of average score distributions of SEQUEST: The probability ratio method. *Molecular & Cellular Proteomics*, *7*(6), 1135–1145. https://doi.org/10.1074/mcp.M700239-MCP200
Nayak, S. R., Joseph, D., Höfner, G., Dakua, A., Athreya, A., Wanner, K. T., Kanner, B. I., & Penmatsa, A. (2023). Cryo-EM structure of GABA transporter 1 reveals substrate recognition and transport mechanism. *Nature Structural & Molecular Biology*, *30*(7), 1023–1032. https://doi.org/10.1038/s41594-023-01011-w
Núñez, E., Alonso-Torres, P., Fornés, A., Aragón, C., & López-Corcuera, B. (2008). The neuronal glycine transporter GLYT2 associates with membrane rafts: Functional modulation by lipid environment. *Journal of Neurochemistry*, *105*(6), 2080–2090. https://doi.org/10.1111/j.1471-4159.2008.05292.x
Núñez, E., Perez-Siles, G., Rodenstein, L., Alonso-Torres, P., Zafra, F., Jiménez, E., Aragon, C., & Lopez-Corcuera, B. (2009). Subcellular localization of the neuronal glycine transporter GLYT2 in brainstem. *Traffic*, *10*(7), 829–843. https://doi.org/10.1111/j.1600-0854.2009.00911.x
Ohno, Y., Kihara, A., Sano, T., & Igarashi, Y. (2006). Intracellular localization and tissue-specific distribution of human and yeast DHHC cysteine-rich domain-containing proteins. *Biochimica et Biophysica Acta*, *1761*(4), 474–483. https://doi.org/10.1016/j.bbalip.2006.03.010
Orsburn, B. C. (2021). Proteome discoverer—A community enhanced data processing suite for protein informatics. *Proteome*, *9*(1), 15. https://doi.org/10.3390/proteomes9010015
Penmatsa, A., Wang, K. H., & Gouaux, E. (2013). X-ray structure of dopamine transporter elucidates antidepressant mechanism. *Nature*, *503*(7474), 85–90. https://doi.org/10.1038/nature12533
Ping, Y.-Q., Mao, C., Xiao, P., Zhao, R.-J., Jiang, Y., Yang, Z., An, W.-T., Shen, D.-D., Yang, F., Zhang, H., Qu, C., Shen, Q., Tian, C., Li, Z.-J., Li, S., Wang, G.-Y., Tao, X., Wen, X., Zhong, Y.-N., … Sun, J.-P. (2021). Structures of the glucocorticoid-bound adhesion receptor GPR97-G(o) complex. *Nature*, *589*(7843), 620–626. https://doi.org/10.1038/s41586-020-03083-w
Rastedt, D. E., Vaughan, R. A., & Foster, J. D. (2017). Palmitoylation mechanisms in dopamine transporter regulation. *Journal of Chemical Neuroanatomy*, *83–84*, 3–9. https://doi.org/10.1016/j.jchemneu.2017.01.002
Rees, M. I., Harvey, K., Pearce, B. R., Chung, S. K., Duguid, I. C., Thomas, P., Beatty, S., Graham, G. E., Armstrong, L., Shiang, R., Abbott, K. J., Zuberi, S. M., Stephenson, J. B., Owen, M. J., Tijssen, M. A., van den Maagdenberg, A. M., Smart, T. G., Supplisson, S., & Harvey, R. J. (2006). Mutations in the gene encoding GlyT2 (SLC6A5) define a presynaptic component of human startle disease. *Nature Genetics*, *38*(7), 801–806. https://doi.org/10.1038/ng1814
Ren, J., Wen, L., Gao, X., Jin, C., Xue, Y., & Yao, X. (2008). CSS-Palm 2.0: An updated software for palmitoylation sites prediction. *Protein Engineering, Design & Selection: PEDS*, *21*(11), 639–644. https://doi.org/10.1093/protein/gzn039
Roth, A. F., Wan, J., Green, W. N., Yates, J. R., & Davis, N. G. (2006). Proteomic identification of palmitoylated proteins. *Methods*, *40*(2), 135–142. https://doi.org/10.1016/j.ymeth.2006.05.026
Sanders, S. S., Martin, D. D. O., Butland, S. L., Lavallée-Adam, M., Calzolari, D., Kay, C., Yates, J. R., 3rd, & Hayden, M. R. (2015). Curation of the mammalian palmitoylome indicates a pivotal role for palmitoylation in diseases and disorders of the nervous system and cancers. *PLoS Computational Biology*, *11*(8), e1004405. https://doi.org/10.1371/journal.pcbi.1004405
Schneider, A., Länder, H., Schulz, G., Wolburg, H., Nave, K.-A., Schulz, J. B., & Simons, M. (2005). Palmitoylation is a sorting determinant for transport to the myelin membrane. *Journal of Cell Science*, *118*(Pt 11), 2415–2423. https://doi.org/10.1242/jcs.02365
Shahsavar, A., Stohler, P., Bourenkov, G., Zimmermann, I., Siegrist, M., Guba, W., Pinard, E., Sinning, S., Seeger, M. A., Schneider, T. R., Dawson, R. J. P., & Nissen, P. (2021). Structural insights into the inhibition of glycine reuptake. *Nature*, *591*(7851), 677–681. https://doi.org/10.1038/s41586-021-03274-z
Song, J., Wang, J., Jozwiak, A. A., Hu, W., Swiderski, P. M., & Chen, Y. (2009). Stability of thioester intermediates in ubiquitin-like modifications. *Protein Science: A Publication of the Protein Society*, *18*(12), 2492–2499. https://doi.org/10.1002/pro.254
Thomas, R. H., Chung, S.-K., Wood, S. E., Cushion, T. D., Drew, C. J. G., Hammond, C. L., Vanbellinghen, J.-F., Mullins, J. G. L., & Rees, M. I. (2013). Genotype-phenotype correlations in hyperekplexia: Apnoeas, learning difficulties and speech delay. *Brain*, *136*(10), 3085–3095. https://doi.org/10.1093/brain/awt207
Vardar, G., Salazar-Lázaro, A., Zobel, S., Trimbuch, T., & Rosenmund, C. (2022). Syntaxin-1A modulates vesicle fusion in mammalian

neurons via juxtamembrane domain dependent palmitoylation of its transmembrane domain. *Elife*, *11*, e78182. https://doi.org/10.7554/eLife.78182

Villarejo-López, L., Jiménez, E., Bartolomé-Martín, D., Zafra, F., Lapunzina, P., Aragón, C., & López-Corcuera, B. (2017). P2X receptors up-regulate the cell-surface expression of the neuronal glycine transporter GlyT2. *Neuropharmacology*, *125*, 99–116. https://doi.org/10.1016/j.neuropharm.2017.07.018

Won, S. J., Cheung See Kit, M., & Martin, B. R. (2018). Protein depalmitoylases. *Critical Reviews in Biochemistry and Molecular Biology*, *53*(1), 83–98. https://doi.org/10.1080/10409238.2017.1409191

Yamashita, A., Singh, S. K., Kawate, T., Jin, Y., & Gouaux, E. (2005). Crystal structure of a bacterial homologue of $Na^+/Cl^-$—Dependent neurotransmitter transporters. *Nature*, *437*(7056), 215–223. https://doi.org/10.1038/nature03978

Yanai, A., Huang, K., Kang, R., Singaraja, R. R., Arstikaitis, P., Gan, L., Orban, P. C., Mullard, A., Cowan, C. M., Raymond, L. A., Drisdel, R. C., Green, W. N., Ravikumar, B., Rubinsztein, D. C., El-Husseini, A., & Hayden, M. R. (2006). Palmitoylation of huntingtin by HIP14 is essential for its trafficking and function. *Nature Neuroscience*, *9*(6), 824–831. https://doi.org/10.1038/nn1702

Yang, J., Pawlyk, B., Wen, X.-H., Adamian, M., Soloviev, M., Michaud, N., Zhao, Y., Sandberg, M. A., Makino, C. L., & Li, T. (2007). Mpp4 is required for proper localization of plasma membrane calcium ATPases and maintenance of calcium homeostasis at the rod photoreceptor synaptic terminals. *Human Molecular Genetics*, *16*(9), 1017–1029. https://doi.org/10.1093/hmg/ddm047

Yeste-Velasco, M., Linder, M. E., & Lu, Y.-J. (2015). Protein S-palmitoylation and cancer. *Biochimica et Biophysica Acta*, *1856*(1), 107–120. https://doi.org/10.1016/j.bbcan.2015.06.004

Zaballa, M.-E., & van der Goot, F. G. (Directors). (2018). The molecular era of protein S-acylation: Spotlight on structure, mechanisms, and dynamics. *Critical Reviews in Biochemistry and Molecular Biology*, *53*(4), 420–451. https://doi.org/10.1080/10409238.2018.1488804

Zafra, F., Gomeza, J., Olivares, L., Aragon, C., & Gimenez, C. (1995). Regional distribution and developmental variation of the glycine transporters GLYT1 and GLYT2 in the rat CNS. *The European Journal of Neuroscience*, *7*(6), 1342–1352.

## SUPPORTING INFORMATION

Additional supporting information can be found online in the Supporting Information section at the end of this article.

**How to cite this article:** Felipe, R., Sarmiento-Jiménez, J., Camafeita, E., Vázquez, J., & López-Corcuera, B. (2024). Role of palmitoylation on the neuronal glycine transporter GlyT2. *Journal of Neurochemistry*, *168*, 2056–2072. https://doi.org/10.1111/jnc.16181